JACS
JOURNAL OF THE AMERICAN CHEMICAL SOCIETY

Article

pubs.acs.org/JACS

Single Lipid Vesicle Assay for Characterizing Single-Enzyme Kinetics of Phospholipid Hydrolysis in a Complex Biological Fluid

Seyed R. Tabaei,[†] Michael Rabe,[†] Henrik Zetterberg,[‡,§] Vladimir P. Zhdanov,[†,∥] and Fredrik Höök*[,†]

[†]Department of Applied Physics, Chalmers University of Technology, Gothenburg, Sweden

[‡]Clinical Neurochemistry Laboratory, Institute of Neuroscience and Physiology, Department of Psychiatry and Neurochemistry, The Sahlgrenska Academy, University of Gothenburg, Mölndal, Sweden

[§]UCL Institute of Neurology, Queen Square, London WC1N 3BG, United Kingdom

[∥]Boreskov Institute of Catalysis, Russian Academy of Sciences, Novosibirsk, Russia

Supporting Information

ABSTRACT: Imaging of individual lipid vesicles is used to track single-enzyme kinetics of phospholipid hydrolysis. The method is employed to quantify the catalytic activity of phospholipase A2 (PLA2) in both pure and complex biological fluids. The measurements are demonstrated to offer a subpicomolar limit of detection (LOD) of human secretory PLA2 (sPLA2) in up to 1000-fold-diluted cerebrospinal fluid (CSF). An additional new feature provided by the single-enzyme sensitivity is that information about both relative concentration variations of active sPLA2 in CSF and the specific enzymatic activity can be simultaneously obtained. When CSF samples from healthy controls and individuals diagnosed with Alzheimer's disease (AD) are analyzed, the specific enzymatic activity is found to be preserved within 7% in the different CSF samples whereas the enzyme concentration differs by up to 56%. This suggests that the previously reported difference in PLA2 activity in CSF samples from healthy and AD individuals originates from differences in the PLA2 expression level rather than from the enzyme activity. Conventional ensemble averaging methods used to probe sPLA2 activity do not allow one to obtain such information. Together with an improvement in the LOD of at least 1 order of magnitude compared to that of conventional assays, this suggests that the method will become useful in furthering our understanding of the role of PLA2 in health and disease and in detecting the pharmacodynamic effects of PLA2-targeting drug candidates.

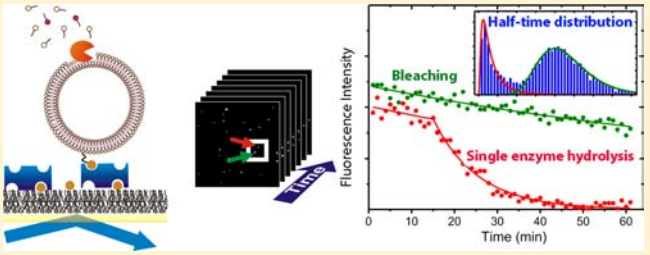

INTRODUCTION

Thanks to the interdisciplinary efforts of biologists, chemists, and physicists during the last few decades, the mechanistic understanding of enzymatic catalysis has advanced dramatically.[1] This is to a significant extent related to advancements in optical microscopy, fluorescent probes, and related conjugation chemistry, which, when combined, have enabled the characterization of the catalytic performance of single enzymes by tracking either the generation of fluorescent products catalyzed by single enzymes or fluorescence emission originating from single enzymes. Historically, the pioneering study in this field was done by Rotman,[2] who proposed to encapsulate individual water-soluble enzymes together with fluorescently active substrate molecules in small-scale liquid droplets. Since then, the field has advanced dramatically (ref 3 and references therein), with new insights regarding the microscopic interpretation of the classical Michaelis−Menten representation of enzyme kinetics[4] and improved limits of detection (LOD) when applied in diagnostic assays[5,6] being two out of many important examples. A complete functional understanding of cell-membrane associated enzymes is, however, still lacking because related studies were performed by employing primarily ensemble-averaging methods. The corresponding studies of single-enzyme kinetics are focused on lipid-bilayer digestion and were so far restricted to the use of individual fluorescently labeled phospholipases.[7,8] To our knowledge, there are no reports on single-enzyme kinetics recorded from unlabeled membrane-bound enzymes, which is a requirement in order to avoid potential side effects from the label or to enable studies of enzymes present in their natural crude biological environment.

In this work, using phospholipase A2 (PLA2) bound to the membrane of lipid vesicles, we present the results of studies of the digestion dynamics of single nanometer-scale phospholipid vesicles by single unlabeled phospholipases in a biological fluid as complex as human cerebrospinal fluid (CSF). Concerning the enzyme used in our work, we recall that PLA2 designates the particularly important A2 subclass of phospholipases, which belongs to a large family of hydrolytic enzymes known to catalyze the digestion of phospholipids at the interface of lipid aggregates such as micelles, monolayers, and bilayers.[9−11] In particular, PLA2 is responsible for the conversion of

Received: May 8, 2013
Published: August 19, 2013

dx.doi.org/10.1021/ja4046313 | J. Am. Chem. Soc. 2013, 135, 14151−14158

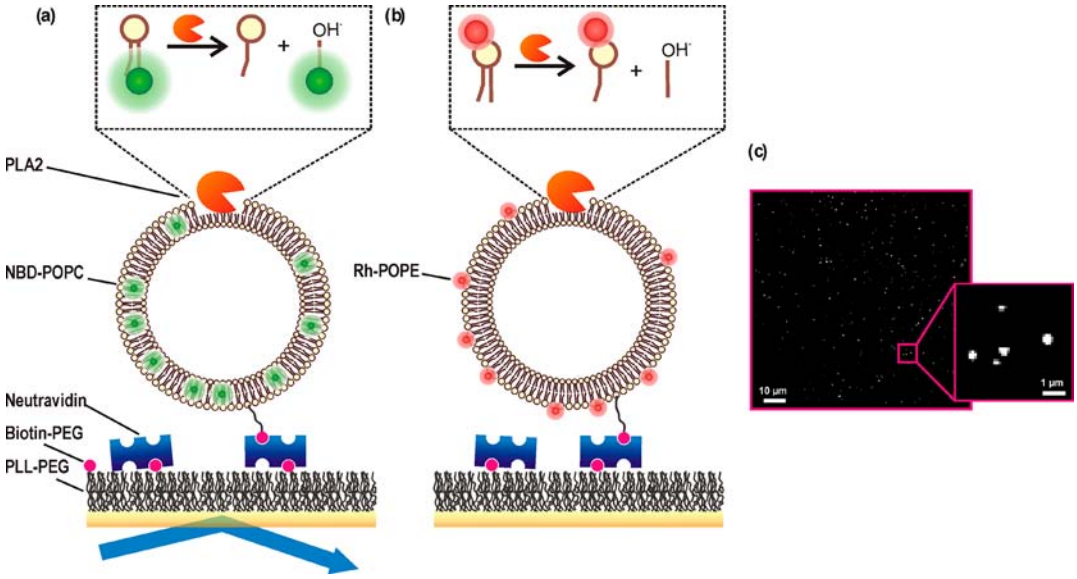

Figure 1. Schematic illustration of the assay for single PLA2 kinetics investigation. Biotinylated POPC (palmitoyl-2-oleoyl-*sn*-glycero-3-phosphocholine) vesicles (diameter of ~90 nm) containing either (a) headgroup-labeled rhodamine-POPE (1 wt %) or (b) chain-labeled phospholipid analogue NBD-POPC (5 wt %) were immobilized on a poly(L-lysine)-grafted-poly(ethylene glycol) (PLL-*g*-PEG) NeutrAvidin (NA)-functionalized PLL-*g*-PEG/PLL-*g*-PEG-biotin-coated glass surface. Phospholipase-mediated hydrolysis of phospholipids was followed by measuring the release of fluorescently labeled products (either rhodamine-lysolipids or NBD-fatty acids) using time-lapse TIRF imaging of around 1000 individual vesicles per field of view. (c) Section (100 μm × 100 μm) of a representative TIRF image and 10-fold magnification showing individual immobilized vesicles.

glycerophospholipids to lysophospholipids and free fatty acids,[12] with the latter being a critical mediator and precursor in inflammation, for example.[13,14] The broad and important biological role of PLA2 becomes apparent from its function as an antimicrobial agent[15,16] as well as observations demonstrating that changes in PLA2 activity and/or the expression level correlate with numerous pathological conditions, such as cancer,[17,18] acute pancreatitis,[19] and coronary heart diseases and ischemic stroke[20,21] plus a broad range of neurodegenerative disorders,[22] such as schizophrenia[23] and Alzheimer's disease.[24,25] Variations in PLA2 activity can accordingly serve as a diagnostic and prognostic disease biomarker, and this and related membrane-associated enzymes have also emerged as potential targets in drug development.[26,27]

Immunological methods such as radioimmunoassays, ELISA, and Western blot have been shown to be sensitive enough to detect relatively low PLA2 levels (typically 10 to 100 pM) in biological samples.[28,29] However, these methods are not sensitive to whether the enzyme is functionally active. Most diagnostic assays are therefore based on direct measurements of PLA2 activity (usually defined as the amount of released product per unit time under conditions at which the conversion rate is not limited by substrate concentrations) by tracing the rate of PLA2-specific product generation upon mixing of artificially produced phospholipid vesicles and a bodily fluid of interest.[30,31] Information about enzyme activity obtained in this way can be translated to specific enzymatic activity, here defined as the substrate conversion rate by a single enzyme, by independently determining the concentration of active enzymes using combinations of immune assays and active-site titration.[32] However, this labor-intensive approach adds uncertainty and provides indirect rather than direct information about the concentration of active enzyme. In this work, we show that by resolving the digestion of individual lipid vesicles by single enzymes simultaneous information about both the specific enzymatic activity and the active enzyme concentration can be obtained in a single experiment at the high sensitivity required for the analysis of PLA2 in a biological sample as complex as CSF.

This was accomplished using total internal reflection fluorescence (TIRF) microscopy, applied to resolve PLA2 digestion of individual surface-immobilized lipid vesicles temporally by recording the PLA2-induced release of fluorescently labeled products. The single-enzyme mode of operation was verified by employing various lines of evidence including a new means to relate the vesicle-size distribution to the distributions of the hydrolysis half-times and lag time of individual vesicles. The detailed design, sensitivity, and overall performance of the assay were optimized using often-employed model enzyme phospholipase A2 from the venom of *Naja mossambica mossambica* (Naja PLA2), which has a structure and catalytic action similar to those of mammalian enzymes.[33] These results were correlated with those obtained using CSF, enabling not only relative but also quantitative PLA2 concentration determinations in CSF, with a sensitivity that is orders of magnitude better than that of conventional ensemble-averaging assays. Motivated by previous work suggesting that neurological disorders are connected to altered PLA2 activity in CSF,[23−25] we further explored whether the single-enzyme mode of detection makes it possible to deduce if these previously observed differences are more likely related to an alteration in enzyme concentration or to specific enzymatic activity. Because many disease states are known to be related to posttranslational protein modifications or mutations that can influence enzymatic activity,[11,34] we envision that a knowledge of the relative influence of these two effects on a measured change in enzyme activity may increase the diagnostic capacity of enzyme-based assays. Such studies are also likely to shed new light on physiological changes behind different diseases involving cell-membrane-associated enzymes, thus providing

dx.doi.org/10.1021/ja4046313 | J. Am. Chem. Soc. 2013, 135, 14151−14158

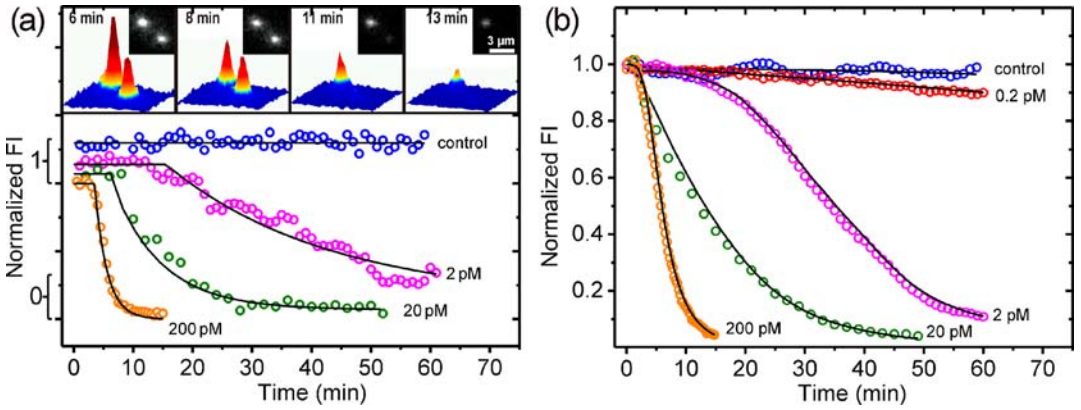

Figure 2. Lipid digestion kinetics on the single vesicle and ensemble levels reveal a subpicomolar LOD. (a) Time traces of the fluorescence emission from a single POPC lipid vesicle labeled with Rh-PE (1%) in the presence of different Naja-PLA2 concentrations in a 20 mM TRIS buffer, pH 7.5, containing 5 mM Ca^{2+}. The top row represents surface plots of the fluorescence intensity of a selected area from typical TIRF images (5 μm × 5 μm) showing two decaying vesicles exposed to Naja PLA2 at 200 pM. The control (open blue circles) represents the response in the absence of Ca^{2+}. (b) Averaged fluorescence intensity traces corresponding to ~1000 individual vesicles, where in addition to the PLA2 concentrations shown in plot a the response obtained at 0.2 pM PLA2 is also shown.

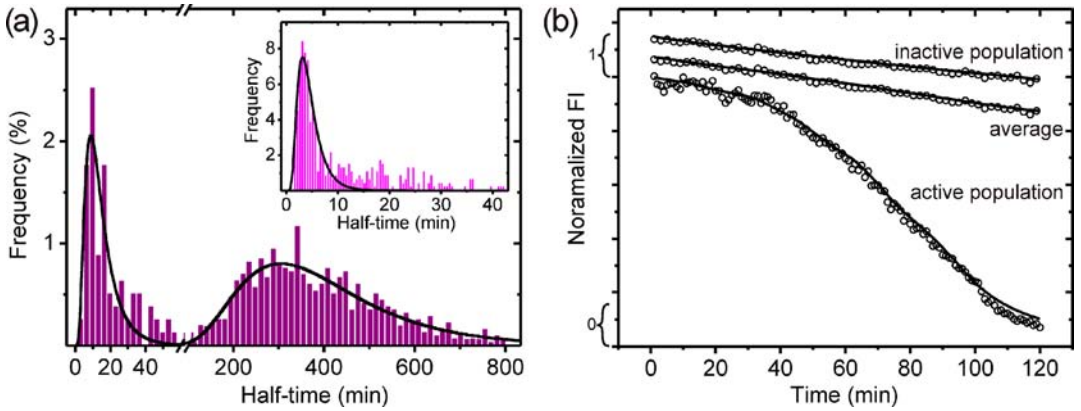

Figure 3. Lipid vesicle digestion kinetics at a subpicomolar enzyme concentration suggest a single-enzyme regime. (a) Histograms of half-times of the fluorescence intensity decay of ~1400 individual vesicles incubated with Naja PLA2 at 0.2 pM. The inset shows the histogram of all half-times corresponding to the activity of Naja PLA2 at 2.0 pM. (b) Averaged fluorescence intensity traces corresponding to the active and inactive populations in plot a. Also shown is the average trace corresponding to the whole ensemble.

pharmaceutically relevant information not easily obtained by other means.

RESULTS

In the first part of this section, we describe the key elements of the single-vesicle assay, such as its capacity to detect subpicomolar concentrations of the model enzyme Naja PLA2 within less than an hour and an argument supporting the assertion that at subpicomolar PLA2 concentrations each digested vesicle is predominantly digested by a single enzyme. In the second part, the assay is applied to detect sPLA2 in CSF, yielding results that further support the single-enzyme hypothesis and showing that in the single-enzyme-per-vesicle regime both the specific enzymatic activity and relative enzyme concentration can be simultaneously and independently determined. The results obtained for CSF from healthy and AD individuals are discussed in light of previous reports correlating the PLA2 activity of human CSF with AD.[24,25,35]

Single-Vesicle/Single-Enzyme Assay. The single-vesicle hydrolysis assay is schematically illustrated in Figure 1, together with a TIRF micrograph of a representative image of immobilized vesicles with typical intervesicle distances of 1 to 5 μm, which enables ~10^3 vesicles to be individually detected in the field of view (190 μm × 190 μm). Upon PLA2 cleavage of fluorescently head- (rhodamine-POPE) or tail-labeled (NBD-POPE) lipids, water-soluble fluorescent cleavage products escape from the lipid membrane and the evanescent volume of the TIR excitation.

To characterize the sensitivity of the assay, a comprehensive set of experiments using different Naja PLA2 concentrations (2 to 200 pM) was performed in the presence of Ca^{2+}, including a control experiment at 20 pM in the absence of Ca^{2+}. Representative temporal variations in fluorescence emission from single vesicles are shown in Figure 2a. High specificity of the assay was verified from the lack of significant changes in the signal in the absence of Ca^{2+}, which is a well-known cofactor for Naja PLA2.[11] In the presence of Ca^{2+}, there was a rapid intensity drop after a concentration-dependent latency period, which decreased from ~30 to ~5 min as the Naja PLA2 concentration was increased from 2 to 200 pM. This so-called lag-burst behavior, which is characterized by a sudden acceleration in the rate of hydrolysis after a concentration-dependent latency time, is a frequently reported characteristics of PLA2[9] and is commonly attributed to a slow accumulation of hydrolysis products, which eventually induces phase-segregated

dx.doi.org/10.1021/ja4046313 | J. Am. Chem. Soc. 2013, 135, 14151−14158

domains and/or altered membrane strain, leading to enhanced enzymatic activity.[36−38]

When the signal for ∼1000 individual vesicles is averaged, the PLA2 activity could be detected with a signal-to-noise (S/N) ratio of ∼500 at a concentration down to 2 pM (Figure 2b), which competes very favorably with both established assays[30] as well as recently demonstrated methods utilizing gold-nanoparticle aggregation for signal enhancement.[39] However, although nearly the entire population of vesicles was digested within ∼60 min at a PLA2 concentration of 2 pM, the signal obtained at 0.2 pM PLA2 was hardly distinguishable from the background signal within this time period. From the appreciable concentration dependence of the latency period (Figure 2a), a reasonable explanation of the weak signal at 0.2 pM is that only a very small fraction of the vesicles have sufficient PLA2 coverage to initiate lag-burst behavior within the experimental time window. Although absent in the ensemble-averaged signal, the single-vesicle resolution of the assay fortunately provides a unique opportunity to characterize whether a fraction of the vesicles indeed displays such lag-burst behavior.

The kinetic traces of all recorded vesicles (∼1400 at 0.2 pM Naja PLA2) were analyzed by fitting them by a piecewise-defined function composed of two concatenated monoexponential decays accounting for the slow initial lag phase and the fast burst phase, respectively (eq 2). This analysis revealed that under these conditions a majority of all recorded vesicles does not show a burst phase. Instead, the observed half-times of these vesicles were on average identical to the half-time of the photobleaching process, indicating the absence of enzymatically active molecules. However, ∼100 vesicles (7%) were identified to show the characteristic lag-burst behavior with short half-times indicative of enzymatic activity. As detailed in the Supporting Information, the time dependence of the lag phase can be attributed to an intrinsic lag time and diffusion-controlled enzyme binding (Figure S3). Figure 3a presents a histogram plot with two maxima corresponding to the two groups with and without enzymatic activity, which in the following text are referred to as active and inactive vesicle population, respectively.

One striking feature that emerges from this way of filtering out active and inactive vesicle populations is that the averaged temporal response of the active population (Figure 3b) displays decay kinetics that are very similar to those obtained at the higher PLA2 concentrations, despite a prolonged latency phase (cf. Figure 2b). In fact, a detailed inspection of the curves in Figure 3b yields a S/N ratio for PLA2 detection at 0.2 pM that differs by more than 20-fold between the total (S/N ≈ 7) and the filtered (S/N ≈ 160) signals. This improvement in the limit of detection obviously makes the concept attractive for diagnostic applications because both low levels and small differences in PLA2 concentration can be detected. In addition, the high sensitivity might make it possible to reduce the sample volume drastically.

It is in this context relevant to stress that an even more appealing feature of the assay becomes clear if one considers the fact that at low enzyme concentrations each of the vesicles of the active population appears to be digested by a single enzyme. Although not previously resolved on the single-vesicle level, it has been concluded from ensemble-averaging measurements of suspended vesicles that at sufficiently low PLA2 to lipid ratios a single nanoscale vesicle can be readily digested by a single enzyme that stays bound to the vesicle during a sufficient number of catalytic cycles.[40] In our case, the single-enzyme regime is visible explicitly because the observation (histograms in Figure 3a) that the reaction occurs only in a small fraction (7%) of vesicles indicates that the main part of the vesicles does not contain enzymes. Assuming a Poisson distribution of enzymes at vesicles and admitting that 93% of vesicles are free of enzymes, we determine that 6.7% contain only one enzyme whereas only 0.3% contain two or more enzymes. The single-enzyme hypothesis is further supported by the fact that the highest possible PLA2 coverage that can be obtained under diffusion-limited conditions at subpicomolar concentrations within these time scales corresponds to less than one enzyme per vesicle (Supporting Information and additional discussion below). Similarly, the anticipated enzyme coverage at the expected low nanomolar affinity prior to the onset of digestion[41] is in agreement with less than one (∼1/10) enzyme per vesicle. It should also be noted that the observed half time of ∼10 min is close to the residence time obtained under relatively similar conditions,[41] albeit in the absence of Ca^{2+}. This suggests that the sudden interruption of vesicle digestion due to enzyme release could be frequent. However, such events (as illustrated in Figure S4 in the Supporting Information) are rare (<10 per 1000 vesicles), indicating that the sudden acceleration in the rate of hydrolysis after the latency time may be, as previously reported, accompanied by increased affinity and a prolonged residence time.[42]

Analysis of PLA2 Activity in Human CSF Samples. Inspired by the utterly low detection limits obtained under single-enzyme detection conditions for Naja PLA2 and the reports suggesting that the PLA2 activity in cerebrospinal fluid (CSF) is altered for patients suffering from AD and schizophrenia, we investigated the possibility of detecting PLA2 activity in human CSF samples. Bearing in mind potential diagnostic applications, we have performed experiments with CSF diluted as 1:10, 1:50, 1:100, and 1:1000 at a Ca^{2+} concentration of 5 mM (Figure 4a).

At a 50-fold dilution and above, there are two clearly separated half-time distributions very similar to those observed in the case of Naja PLA2 at 0.2 pM (cf. Figure 2), suggesting one active and one inactive vesicle population. In addition, the fluorescence traces belonging to the vesicles of the active population showed characteristic lag-burst kinetics, whereas the traces of the inactive population showed a slow monoexponential decay being attributed to photobleaching. The latter interpretation was verified by inhibiting the predominantly existing secretory PLA2 (sPLA2) being present in human CSF[24] by using sPLA2 specific inhibitor thioetheramide-PC. As shown in the inset of Figure 4a, the active population, which was clearly pronounced in the absence of the inhibitor, transformed into an entirely inactive population. This thus confirms that the inactive population corresponds to photobleaching and that the active population corresponds to sPLA2 digestion.

The characteristic bimodal distribution of half-times observed above the 50-fold dilution suggests that the active population corresponds to single-enzyme digestion. This interpretation gains additional support from the vesicle-size dependence of the sPLA2-mediated hydrolysis half-times illustrated in Figure 4b, which shows histograms of the half-times obtained for two vesicle subpopulations with diameters smaller than ∼80 nm (black bars) or larger than ∼120 nm (gray bars), both of which are selected from the active population on the basis of the established correlation between

dx.doi.org/10.1021/ja4046313 | J. Am. Chem. Soc. 2013, 135, 14151−14158

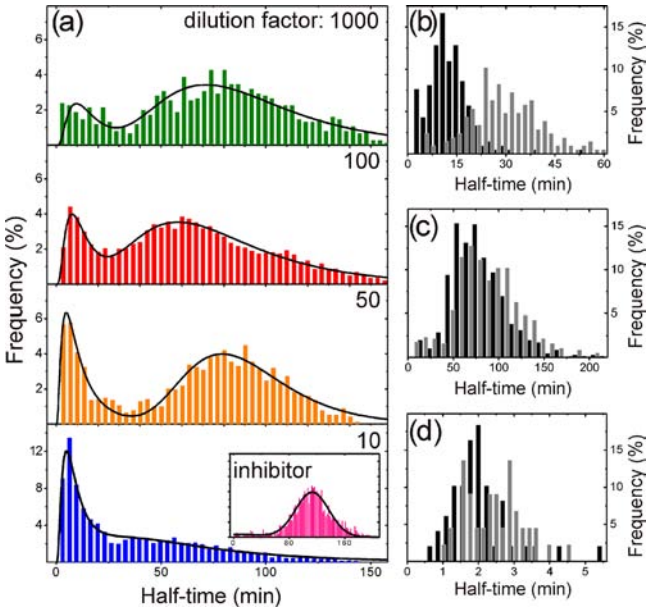

Figure 4. Single-enzyme kinetics measured in human cerebrospinal fluid. (a) Histograms of hydrolysis half-times of individual vesicles generated by PLA2-containing CSF at various dilutions (1:10, 1:50, 1:100, and 1:1000), revealing one active and one inactive population. The histogram in the inset depicts the hydrolysis half-times of the 100-fold-diluted CSF sample in the presence of sPLA2 inhibitor thioetheramide-PC at a concentration of 2 μM, verifying that the fast and slow populations represent vesicles that are either digested or not. The distributions of the reaction half-times for two subpopulations of vesicles of different size (see the text) are shown for the active population of the 100-fold-diluted CSF sample in part b, the inactive population of 100-fold CSF sample in part c, and the active population obtained for Naja PLA2 at 200 pM in part d. The vesicle fluorescence intensity together with the vesicle size distribution measured by nanoparticle tracking (NTA) was used to estimate the vesicle size. (See Supporting Information Figures S1 and S2 for the generation of plots b–d.) PLA2 in CSF was incapable of digesting headgroup-labeled phospholipids. Activity was observed only for vesicles containing acyl-chain-labeled phospholipids such as NBD-PC. Therefore, all experiments on human CSF samples were conducted on surface-tethered vesicles containing 5% NBD-PC as a marker.

fluorescence intensity and vesicle size[43] (Supporting Information Figure S1). The reaction half-time of the active population is clearly size-dependent (Figure 4b), but the same analysis of the inactive population displays no size dependence (Figure 4c). The clear correlation between the reaction half-time and vesicle area ($\propto$ lipid content) is consistent with single-enzyme digestion, unless the enzyme coverage (number of bound enzymes per membrane area) displays a strong vesicle-size dependence. The latter suspicion is indeed valid because it has been shown that the coverage of certain membrane-binding proteins displays a strong vesicle-size dependence.[44] In the case of PLA2, however, the vesicle-size-dependent enzyme coverage is minor, as verified by the absence of a size-dependent hydrolysis half-time at a 200 pM Naja PLA2 concentration (Figure 4d), in which case the digestion occurs in a multiple-enzyme-per-vesicle mode (cf. the absence of a bimodal half-time distribution shown in the inset of Figure 2a).

Additional support for the single-enzyme mode can be gained by comparing the observed half-time distribution to that expected by taking the vesicle-size distribution into account. The reaction half-time is expected to be proportional to the area of the vesicles (i.e., $\tau = Ar^2$, where r is the vesicle radius and A is a constant). This relation allows us to express the half-time distribution, $f(\tau)$, via the vesicle size distribution, $F(r)$, by using the conventional rule of changing variables,

$$f(\tau) = F(r(\tau))\,\frac{\mathrm{d}r(\tau)}{\mathrm{d}\tau} \qquad (1)$$

where $\mathrm{d}r(\tau)/\mathrm{d}\tau = 1/[2(A\tau)^{1/2}]$. Figure 5a shows the experimentally obtained size distribution of the vesicles (CSF 100× dilution) of the active subpopulation measured by TIRF microscopy (orange columns). The histogram was fitted by an appropriate empirical function ($F(r)$, solid line), which was used to calculate the expected half-time distribution based on eq 1. Figure 5b depicts both the calculated and the experimental half-time distributions (solid lines and red columns, respectively). The excellent overlap obtained between predicted and measured half-time distributions is consistent with the hypothesis that each vesicle belonging to the active population is predominantly digested by a single enzyme.

Exploration of the Diganostic Potential of the Single-Enzyme Assay. The enzymatic activity determined in

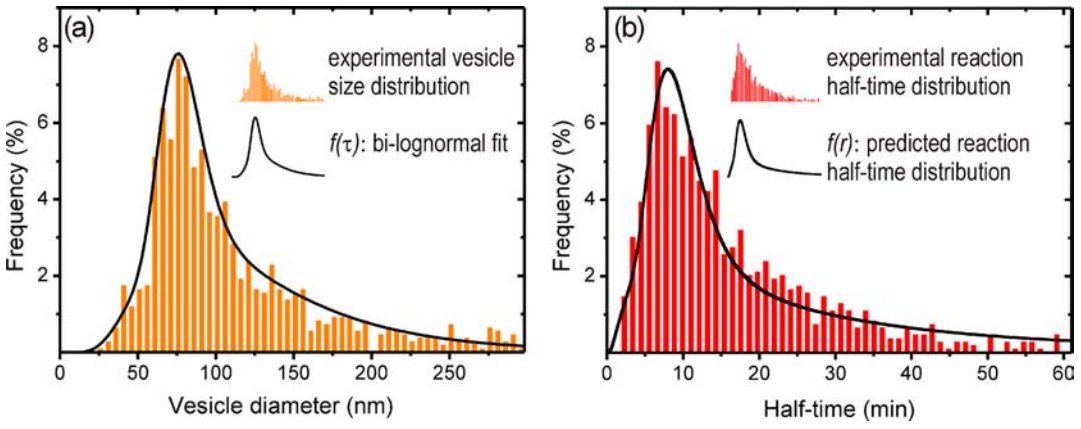

Figure 5. Analysis of the half-time distribution vs vesicle size to strengthen the single-enzyme hypothesis. (a) The size distribution of all vesicles from the active subpopulation of a CSF sample (100× diluted) is measured by TIRF microscopy (orange columns) and fitted by a bilognormal function (solid line). (b) The fitted function is used as an input to calculate the expected probability density function of the half-time distribution (solid line). The expected function agrees very well with the measured half-time distribution (red columns).

dx.doi.org/10.1021/ja4046313 | J. Am. Chem. Soc. 2013, 135, 14151–14158

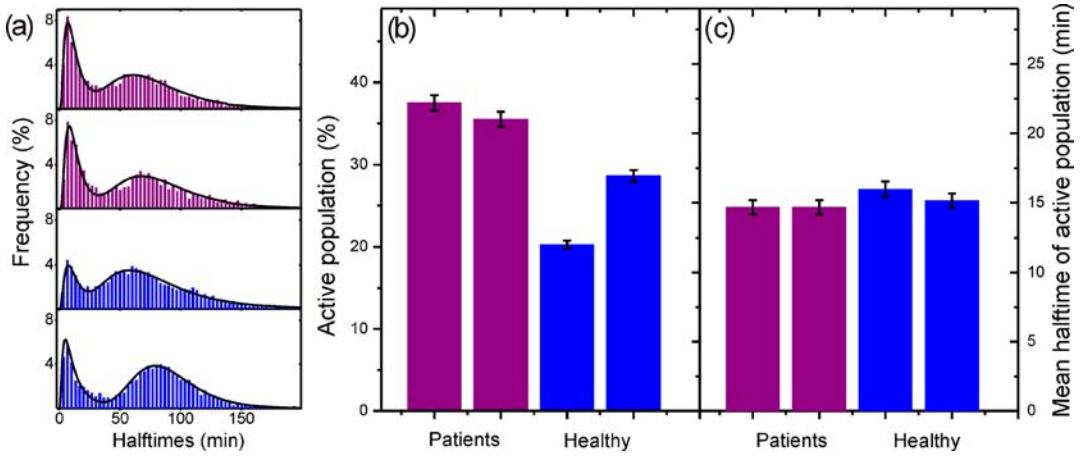

Figure 6. Comparison of PLA2 digestions between AD patients and healthy controls. (a) Histograms of hydrolysis half-times of individual vesicles generated by CSF (1:100) from AD patients (red) and healthy individuals (blue). (b) Percentage of active populations in patients and healthy controls. (c) Mean half-time of active populations in patients and healthy samples.

conventional ensemble measurements depends on the maximum turnover number, k_{cat}, and the Michaelis–Menten constant, K_m, characterizing the rate of product formation and the affinity between the enzyme and the substrate, respectively, as well as the enzyme and substrate concentrations. With a single enzyme being responsible for the digestion of a single vesicle, the enzyme concentration does not influence the measured rate (or half-time, as used in the present analysis) but rather the relative proportion between active and inactive vesicle populations. This is clear from a more detailed inspection of the histograms representing different CSF dilutions in Figure 4a, which reveals that the percentage of the active population depends on the CSF dilution factor whereas the mean half-time is essentially independent of this factor, at least for dilutions of 50-fold or higher (i.e., where the single-enzyme mode is expected to dominate). Hence, although K_m and k_{cat} would be accessible only through an advanced nonlinear regression analysis,[45] the mean half-time represents a specific enzymatic activity of a single enzyme, and the ratio of the active and inactive vesicle populations represents the enzyme concentration. This means that the assay gives simultaneous information about two parameters, reflecting the specific PLA2 activity on the one hand and the relative enzyme concentration on the other hand.

With this information readily at hand, we were curious to determine whether the assay would be sensitive enough to tell if the previously reported variations in PLA2 activity of AD patients[24,25] depend on the altered specific enzymatic activity due to pathological mutations or post-translational modifications or an altered expression level, which leads to changes in the PLA2 concentration. In this proof-of-principle study, we have explored two samples from AD patients and two from healthy controls. Although this does not allow us to draw statistically secured conclusions, it is interesting to note that the enzyme concentration, estimated as the ratio of the active population to all vesicles (Figure 6a), appears to differ by up to 56% (Figure 6b). In contrast, the specific enzymatic activity, estimated as the mean of the active half-time distribution (Figure 6a), is preserved within 7% in the four different CSF samples (Figure 6c). These results indicate that previously reported differences in PLA2 activity in CSF samples from healthy and AD individuals originate from differences in expression levels rather than from the altered enzymatic activity.

DISCUSSION

In this work, an ultrasensitive assay providing real-time measurements of PLA2 activity at the single-enzyme level in complex physiological samples was introduced. The high sensitivity allowed us to detect the enzyme activity in samples containing subpicomolar PLA2 concentrations within less than an hour. This was accomplished using arrays of surface-attached fluorescently labeled single vesicles acting as substrates for PLA2. Using time-lapse TIRF microscopy, we imaged the tethered vesicles individually, allowing statistics of lipid digestion to be obtained for up to several thousand vesicles in one experiment. We have demonstrated that the single-vesicle analysis is a key factor in boosting the sensitivity below the picomolar limit basically because image analysis can be used to discard unwanted signals from vesicles that are not digested. This was implemented in software that enabled the automatic analysis of the lag-burst kinetics that is characteristic of phospholipase activity.

The single-vesicle/enzyme measurements allowed the simultaneous determination of concentration and specific enzyme activity variations between different samples. This unique feature was used to compare the PLA2 activities of CSF samples from individuals diagnosed with AD and healthy controls. Our analysis suggests that the observed differences in the CSF PLA2 activity of AD patients and healthy individuals originate from a variation in the PLA2 concentration rather than an alteration in the specific activity of the enzyme. For the small number of human samples used, this conclusion remains preliminary in a medical diagnostics context but strongly encourages extended studies to be undertaken in forthcoming work. It is also interesting to note that the specific enzymatic activities of Naja PLA2 and sPLA2 in CSF appear to be very similar and that a dilution factor of 100 appears to yield a response that is similar to that obtained at 0.2 pM Naja PLA2. This thus suggests that sPLA2 concentrations in CSF are in the low picomolar range, which is in agreement with the previous concentration determination of PLA2 in bodily fluids.[46]

Diagnostic assays do not generally require quantitative estimates of absolute concentrations but are equally reliable if based on relative differences. As such, the assay at this stage is

dx.doi.org/10.1021/ja4046313 | J. Am. Chem. Soc. 2013, 135, 14151–14158

already suitable for more large-scale screening applications, although such a step would benefit significantly from improvements in liquid handling using microfluidics or robotic dispensing. Future work will concentrate on exploring the possibility of applying the assay for improved diagnostics, not only for AD but also for other disease states that are known to be related to altered phospholipase activity. PLA2 is present in many human bodily fluids including serum, synovial fluid, urine, seminal plasma, and tear fluid,[11] and we envision an expansion of the study to investigations of these types of biological matrices and associated disease states.

MATERIALS AND METHODS

Vesicle Preparation. Small unilamellar vesicles were made by the extrusion method. Briefly, a solution of POPC(1-palmitoyl-2-oleoyl-*sn*-glycero-3-phosphocholine), DSPE-PEG(2000)biotin(1,2-distearoyl-*sn*-glycero-3-phosphoethanolamine-*N*-[biotinyl(poly(ethylene glycol))-2000] (0.1 mol %), and either 1 wt % rhodamine-PE(1,2-dioleoyl-*sn*-glycero-3-phosphoethanolamine-*N*-(lissamine rhodamine B sulfonyl) or 5 wt % NBD-PC(1-palmitoyl-2-{6-[(7-nitro-2-1,3-benzoxadiazol-4-yl)amino]hexanoyl}-*sn*-glycero-3-phosphocholine) in chloroform was first dried using a flow of nitrogen. (All lipids were purchased from Avanti Polar Lipids.) The dried lipid film was stored in vacuum for 3 h, after which it was rehydrated with either Tris-HCl 20 mM, KCl 100 mM, pH 7.4 or Tris-HCl 100 mM, KCl 50 mM, pH 7.4. After vortex mixing of the solution of hydrated lipids (4 mg/mL), unilamellar vesicles were made with a miniextruder (Avanti Polar Lipids) using a polycarbonate membrane (100 nm pore size, Avanti Polar Lipids). The vesicle size distribution was measured by the Nano-Sight particle-tracking technique (NanoSight, U.K.).

CSF Samples. The use of human CSF samples was approved by the ethics committee of the University of Gothenburg. CSF samples were collected by lumbar puncture through the L3/L4 or L4/L5 interspace. The first 12 mL of CSF was collected in a polypropylene tube and immediately transported to the local laboratory for centrifugation at 2000*g* at 4 °C for 10 min. The supernatant was pipetted off, gently mixed to avoid possible gradient effects, and separated into 2−5 mL aliquots that were stored at −80 °C pending testing. The samples were from patients who sought medical advice because of cognitive impairment. Patients were designated as normal or AD according to CSF biomarker levels using cutoffs that are >90% specific for AD:[47,47] total tau (T-tau) >350 ng/L, phospho-tau (P-tau) >80 ng/L, and Aβ42 <530 ng/L. None of the biochemically normal subjects fulfilled these criteria. CSF T-tau, P-tau, and Aβ42 levels were determined in a clinical routine using commercially available enzyme-linked immunosorbent assays (INNOTEST, Innogenetics, Ghent, Belgium) by board-certified laboratory technicians following protocols approved by the Swedish Board for Accreditation and Conformity Assessment (SWEDAC).

Single-Vesicle Hydrolysis Assay. Glass microscope coverslips were first sonicated in SDS (1%), followed by rinsing with Milli-Q water. Next, they were treated with UV ozone for 20 min. The coverslips were coated by a self-assembled monolayer of a 10 00:1 mixture of poly(L-lysine)-*grafted*-poly(ethylene glycol) (PLL-*g*-PEG) and PLL-*g*-PEG(-biotin) (SuSoS AG, Switzerland). The biotin-modified PEGylated surface was further incubated with neutravidin (10 μg/mL) for 20 min and subsequently washed carefully. Biotinylated POPC vesicles were immobilized at a concentration of 0.1 μg/mL for 10 min. During TIRF measurements, surface-bound vesicles were incubated with PLA2 samples from either Naja mossambica mossambica (Sigma) or human CSF. Prior to use, the samples were diluted in Tris-HCl 100 mM, KCl 50 mM, $CaCl_2$ 5 mM, pH 7.4. All measurements were conducted in a cell designed to have stationary conditions in a liquid reservoir that is connected to a slow laminar flow at its upper end. Therefore, we used a 300-μm-thick Teflon ring mounted on the glass substrate. To avoid complete depletion of the reservoir from enzymes and to ensure a constant temperature within the cell, we applied a constant flow of 25 μL/min to exchange the solution at a distance 300 μm above the sensor surface (the time scale of this step was 6 min). In particular, this setup allowed us to exchange the buffer solution at the onset of each experiment efficiently by applying a fast, nonlaminar flow (~10 mL/min), followed by enzyme binding controlled by diffusion under stationary conditions. The measurements were conducted at 37 ± 1 °C in the case of the human CSF samples or at room temperature in the case of Naja PLA2 samples, respectively.

TIRF Microscopy. Total internal reflection fluorescence (TIRF) microscopy was performed on an inverted Eclipse TE 2000 microscope (Nikon) equipped with a high-pressure mercury lamp, an Apo TIRF 60× oil objective (NA 1.49), and a Luca EMCCD camera (1002 × 1004 pixel). Filter sets and dichroic mirrors in the filter cubes were chosen to match the excitation and emission properties of the selected fluorophores. Images (190 μm × 190 μm) were acquired for 200 ms in time intervals of 15 or 60 s.

Single-Vesicle Analysis. The single-vesicle analysis procedure was conducted in Matlab 2010 (scripts available upon request). All TIRF images within one data set were corrected for lateral drifts and for the background signal. Subsequently, the positions of all recorded vesicles were determined using the first image as the reference image. A vesicle was defined as a group of at least three connected pixels exceeding an intensity threshold of three times the average noise level. Intensity time traces of the vesicles were obtained by pixelwise integration of the intensity over their specific surface area in all images of the data set. Subsequently, these kinetic traces were used to allocate vesicles to the active or inactive population, respectively, in the following way. Kinetic traces that showed the characteristic lag-burst behavior, comprising a very slow intensity decrease in the beginning followed by a sudden and fast intensity decay after a certain lag phase, were attributed to vesicles of the active population. In the case of low PLA2 concentrations (0.2 pM for Naja-PLA2, 100-fold dilutions for human CSF samples), the activity corresponded to the fast decay period and was mostly a result of one enzyme. Vesicles whose kinetic traces did not show the characteristic lag-burst feature but only a slow decay over the whole measurement period contained no enzyme and were allocated to the inactive population. To quantify the vesicle hydrolysis process, the kinetics of all vesicles of the active population were fitted by two concatenated monoexponential functions with rate constants describing the photobleaching process (k_{bl}) during the lag phase and the lipid hydrolysis process (k_{hyd}) during the burst phase,

$$I(t) = \begin{cases} I(0)\exp(-k_{bl}t) & t < t_{lag} \\ I(t_{lag})\exp[-k_{hyd}(t-t_{lag})] & t \geq t_{lag} \end{cases} \quad (2)$$

In this expression at $t > t_{lag}$, the rate constant k_{hyd} formally characterizes hydrolysis and photobleaching occurring in parallel. However, the photobleaching is slow ($k_{bl} < k_{hyd}/10$), and k_{hyd} can be used as a measure of the reaction rate. In the case of a single enzyme per vesicle, k_{hyd} is a measure of the enzyme activity. The corresponding reaction half-time is defined as $\tau = \ln 2/k_{hyd}$. Histograms of reaction half-times were normalized with respect to the number of analyzed vesicles and fitted by a log-normal distribution, giving rise to the mean half-time.

With 0.1 mol % DSPE-PEG(2000)biotin, each vesicle can be bound to the surface with up to around 100 linkers. Because one linker is sufficient for vesicle attachment, vesicle removal due to digestion of the DSPE headgroup is expected to be a relatively unlikely event. However, when sudden vesicle removal occurs, it can be easily distinguished from gradual lipid digestion. Instead of a gradual decrease in the time evolution of the fluorescence emission, a sudden stepwise decrease is observed (Figure S4 in Supporting Information). Such events are relatively common (~5% of all vesicles) but were excluded from the analysis. Similarly, the rare events (<1%) corresponding to enzyme release were excluded from the analysis.

dx.doi.org/10.1021/ja4046313 | J. Am. Chem. Soc. 2013, 135, 14151−14158

■ ASSOCIATED CONTENT

Supporting Information

Detailed descriptions of the vesicle size determination and the correlation between hydrolysis half-time and vesicle size. Analysis of diffusion-limited enzyme binding, the lag-time distribution in the single-enzyme-per-vesicle mode, and an illustration of rare events. This material is available free of charge via the Internet at http://pubs.acs.org.

■ AUTHOR INFORMATION

Corresponding Author

fredrik.hook@chalmers.se

Notes

The authors declare no competing financial interest.

■ ACKNOWLEDGMENTS

The Swedish Governmental Agency for Innovation Systems (VINNOVA), the Swedish Research Council, and the Swedish Strategic Research Foundation (SSF) provided financial support for this work.

■ REFERENCES

(1) Ringe, D.; Petsko, G. A. *Science* **2008**, *320*, 1428.
(2) Rotman, B. *Proc. Natl. Acad. Sci. U.S.A.* **1961**, *47*, 1981.
(3) Gorris, H. H.; Walt, D. R. *Angew. Chem., Int. Ed.* **2010**, *49*, 3880.
(4) English, B. P.; Min, W.; van Oijen, A. M.; Lee, K. T.; Luo, G. B.; Sun, H. Y.; Cherayil, B. J.; Kou, S. C.; Xie, X. S. *Nat. Chem. Biol.* **2006**, *2*, 87.
(5) Rissin, D. M.; Kan, C. W.; Campbell, T. G.; Howes, S. C.; Fournier, D. R.; Song, L.; Piech, T.; Patel, P. P.; Chang, L.; Rivnak, A. J.; Ferrell, E. P.; Randall, J. D.; Provuncher, G. K.; Walt, D. R.; Duffy, D. C. *Nat. Biotechnol.* **2010**, *28*, 595.
(6) Li, Z.; Hayman, R. B.; Walt, D. R. *J. Am. Chem. Soc.* **2008**, *130*, 12622.
(7) Rocha, S.; Hutchison, J. A.; Peneva, K.; Herrmann, A.; Muellen, K.; Skjot, M.; Jorgensen, C. I.; Svendsen, A.; De Schryver, F. C.; Hofkens, J.; Uji-I, H. *ChemPhysChem* **2009**, *10*, 151.
(8) Gudmand, M.; Rocha, S.; Hatzakis, N. S.; Peneva, K.; Mullen, K.; Stamou, D.; Uji-I, H.; Hofkens, J.; Bjornholm, T.; Heimburg, T. *Biophys. J.* **2010**, *98*, 1873.
(9) Verger, R.; Mieras, M. C. E.; Dehaas, G. H. *J. Biol. Chem.* **1973**, *248*, 4023.
(10) Scott, D. L.; White, S. P.; Otwinowski, Z.; Yuan, W.; Gelb, M. H.; Sigler, P. B. *Science* **1990**, *250*, 1541.
(11) Dennis, E. A.; Cao, J.; Hsu, Y. H.; Magrioti, V.; Kokotos, G. *Chem. Rev.* **2011**, *111*, 6130.
(12) Verheij, H. M.; Slotboom, A. J.; Dehaas, G. H. *Rev. Physiol., Biochem. Pharmacol.* **1981**, *91*, 91.
(13) Balsinde, J.; Balboa, M. A.; Insel, P. A.; Dennis, E. A. *Annu. Rev. Pharmacol. Toxicol.* **1999**, *39*, 175.
(14) Murakami, M.; Nakatani, Y.; Atsumi, G.; Inoue, K.; Kudo, I. *Crit. Rev. Immunol.* **1997**, *17*, 225.
(15) Harwig, S. S. L.; Tan, L.; Qu, X. D.; Cho, Y.; Eisenhauer, P. B.; Lehrer, R. I. *J. Clin. Invest.* **1995**, *95*, 603.
(16) Nevalainen, T. J.; Graham, G. G.; Scott, K. F. *Biochim. Biophys. Acta, Mol. Cell Biol. Lipids* **2008**, *1781*, 1.
(17) Yamashita, S.; Yamashita, J.; Sakamoto, K.; Inada, K.; Nakashima, Y.; Murata, K.; Saishoji, T.; Nomura, K.; Ogawa, M. *Cancer* **1993**, *71*, 3058.
(18) Park, J. B.; Lee, C. S.; Jang, J. H.; Ghim, J.; Kim, Y. J.; You, S.; Hwang, D.; Suh, P. G.; Ryu, S. H. *Nat. Rev. Cancer* **2012**, *12*, 782.
(19) Nevalainen, T. J. *Am. J. Surg.* **2007**, *194*, S28.
(20) Oei, H. H. S.; van der Meer, I. M.; Hofman, A.; Koudstaal, P. J.; Stijnen, T.; Breteler, M. M. B.; Witteman, J. C. M. *Circulation* **2005**, *111*, 570.
(21) Vasan, R. S. *Circulation* **2006**, *113*, 2335.
(22) Sun, G. Y.; Shelat, P. B.; Jensen, M. B.; He, Y.; Sun, A. Y.; Simonyi, A. *Neuromol. Med.* **2010**, *12*, 133.
(23) Gattaz, W. F.; Hubner, C. V.; Nevalainen, T. J.; Thuren, T.; Kinnunen, P. K. J. *Biol. Psychiatry* **1990**, *28*, 495.
(24) Chalbot, S.; Zetterberg, H.; Blennow, K.; Fladby, T.; Grundke-Iqbal, I.; Iqbal, K. *Clin. Chem.* **2009**, *55*, 2171.
(25) Smesny, S.; Stein, S.; Willhardt, I.; Lasch, J.; Sauer, H. *J. Neural Transm.* **2008**, *115*, 1173.
(26) Magrioti, V.; Kokotos, G. *Expert Opin. Ther. Pat.* **2010**, *20*, 1.
(27) Reid, R. C. *Curr. Med. Chem.* **2005**, *12*, 3011.
(28) Sakamoto, K.; Arakawa, H.; Yamashita, S. I.; Mizuta, H.; Takaki, K.; Ogawa, M. *Res. Commun. Chem. Pathol. Pharmacol.* **1992**, *76*, 279.
(29) Eskola, J. U.; Nevalainen, T. J.; Lovgren, T. N. E. *Clin. Chem.* **1983**, *29*, 1777.
(30) Radvanyi, F.; Jordan, L.; Russomarie, F.; Bon, C. *Anal. Biochem.* **1989**, *177*, 103.
(31) Thuren, T.; Virtanen, J. A.; Lalla, M.; Kinnunen, P. K. J. *Clin. Chem.* **1985**, *31*, 714.
(32) Rotticci, D.; Norin, T.; Hult, K.; Martinelle, M. *Biochim. Biophys. Acta, Mol. Cell Biol. Lipids* **2000**, *1483*, 132.
(33) Kini, R. M. *Toxicon* **2003**, *42*, 827.
(34) Gregory, A.; Westaway, S. K.; Holm, I. E.; Kotzbauer, P. T.; Hogarth, P.; Sonek, S.; Coryell, J. C.; Nguyen, T. M.; Nardocci, N.; Zorzi, G.; Rodriguez, D.; Desguerre, I.; Bertini, E.; Simonati, A.; Levinson, B.; Dias, C.; Barbot, C.; Carrilho, I.; Santos, M.; Malik, I.; Gitschier, J.; Hayflick, S. J. *Neurology* **2008**, *71*, 1402.
(35) Chalbot, S.; Zetterberg, H.; Blennow, K.; Fladby, T.; Grundke-Iqbal, I.; Iqbal, K. *Neurosci. Lett.* **2010**, *478*, 179.
(36) Mouritsen, O. G.; Andresen, T. L.; Halperin, A.; Hansen, P. L.; Jakobsen, A. F.; Jensen, U. B.; Jensen, M. O.; Jorgensen, K.; Kaasgaard, T.; Leidy, C.; Simonsen, A. C.; Peters, G. H.; Weiss, M. *J. Phys.: Condens. Matter* **2006**, *18*, S1293.
(37) Berg, O. G.; Gelb, M. H.; Tsai, M. D.; Jain, M. K. *Chem. Rev.* **2001**, *101*, 2613.
(38) Zhdanov, V. P.; Hook, F. *Biophys. Chem.* **2012**, *170*, 17.
(39) Aili, D.; Mager, M.; Roche, D.; Stevens, M. M. *Nano Lett.* **2011**, *11*, 1401.
(40) Berg, O. G.; Yu, B. Z.; Rogers, J.; Jain, M. K. *Biochemistry* **1991**, *30*, 7283.
(41) Stahelin, R. V.; Cho, W. H. *Biochemistry* **2001**, *40*, 4672.
(42) Jain, M. K.; Egmond, M. R.; Verheij, H. M.; Apitzcastro, R.; Dijkman, R.; Dehaas, G. H. *Biochim. Biophys. Acta* **1982**, *688*, 341.
(43) Kunding, A. H.; Mortensen, M. W.; Christensen, S. M.; Bhatia, V. K.; Makarov, I.; Metzler, R.; Stamou, D. *Biophys. J.* **2011**, *101*, 2693.
(44) Hatzakis, N. S.; Bhatia, V. K.; Larsen, J.; Madsen, K. L.; Bolinger, P. Y.; Kunding, A. H.; Castillo, J.; Gether, U.; Hedegard, P.; Stamou, D. *Nat. Chem. Biol.* **2009**, *5*, 835.
(45) Duggleby, R. G. *Enzyme Kinet. Mech.* **1995**, *D249*, 61.
(46) Nevalainen, T. J.; Kortesuo, P. T.; Rintala, E.; Marki, F. *Clin. Chem.* **1992**, *38*, 1824.
(47) Hansson, O.; Zetterberg, H.; Buchhave, P.; Londos, E.; Blennow, K.; Minthon, L. *Lancet Neurol.* **2006**, *5*, 228.